IEEE Access
Multidisciplinary | Rapid Review | Open Access Journal

SPECIAL SECTION ON WIRELESS BODY AREA NETWORKS

Received August 26, 2018, accepted September 20, 2018, date of publication September 28, 2018, date of current version October 19, 2018.

Digital Object Identifier 10.1109/ACCESS.2018.2872746

An Individual Differentiated Coexisting Mechanism for Multiple Wireless Body Area Networks Based on Game Theory

BING ZHANG AND YU ZHANG
State Key Laboratory of Integrated Services Networks, Xidian University, Xi'an 710071, China
Corresponding author: Bing Zhang (bzhang@mail.xidian.edu.cn)

This work was supported in part by the National High-tech Research and Development Program (863 Program) of China under Grant 2011AA01A106 and in part by the National Key Technology Research and Development Program of China under Grant 2012BAH02B02.

ABSTRACT Wireless body area network (WBAN) is an emerging technology that has enormous potential to be implemented in medical applications. However, the performance of WBANs can be severely degraded by concomitant inter-WBAN interference in some specific environments, where the multiple WBANs are densely deployed, e.g., hospitals and senior citizen communities. In this paper, a novel coexisting mechanism is proposed to deal with the multi-WBANs coexisting which can provide differentiated communication QoS for different WBANs according to their own priority conditions. The proposed mechanism consists of four parts which are time slot allocation, access control, active part interleaving, and power control. Specifically, the time slot allocation is designed based on the game theory. Access control and Active period scheduling are designed referring to the coexisting methods specified in IEEE 802.15.6 standard. In addition, the power control utilizes mobility prediction to adjust transmitting power for each coexisting WBAN. The simulation results demonstrate that the proposed mechanism is stable and convergent in varying coexisting scenarios and can realize differentiated time slot allocation depending on WBANs' priority conditions. Furthermore, when compared with the original mechanisms specified in IEEE 802.15.6, transmission performance of coexisting WBANs is improved in terms of transmission outage probability, transmission energy efficiency, and overall throughput.

INDEX TERMS Wireless body area networks, priority, coexisting, game theory.

I. INTRODUCTION

Wireless Body Area Network is an emerging short range wireless communication technology in the vicinity of human body. It has enormous potential to be implemented in medical applications such as ubiquitous health care, medical treatment and elder monitoring [1]–[3]. In general, a WBAN consists of several sensor nodes deployed on/around or implanted inside the human body, and a central controller called coordinator/hub. Sensor nodes collect certain types of sensing information from human body such as brain electrical activities, blood pressure, core temperature, oxygen saturation, carbon dioxide concentration, etc [4]. The coordinator, which is usually the device like mobile phone or Pad, acts as central controller to collect all the information attained by the sensors and transmit the sensed data to the user or the remote server for further processing.

With the increasing trend for pervasive use of WBAN, several BANs equipped on human body may stay closed to each other resulting in inter-BAN interference. For example in hospital or senior citizen communities, it appears commonly that multiple WBAN-equipped users, as patients or seniors, stay in a room and cause mutual interference. According to the literature [5], without coordination among coexisting WBANs, the transmission performance (e.g. reliability, delay, energy efficiency) of a WBAN will be severely affected by another coexisting WBAN. The degradation will be worse if more WBANs stay close to each other in a limited space. On the other hand, it is not realistic to deploy a centralized controller for these coexisting WBANs to coordinate with each other due to their high mobility feature [6]. As a consequence, in medical application perspective of WBANs, one of the most important issues is the coexistence of multiple WBANs in the vicinity of each other. What's more, considering the mobility attribute of WBANs, the coexistence mechanism should be better in distributed manner.

To deal with the coexisting conditions and mitigate the inter-network interference, several methods have been developed for wireless networks. CSMA/CA and Aloha can be

firstly considered to handle the multi-network transmission due to their easy scalability and operability. Several mechanisms could be found in previous literatures to deal with inter-network interference based on CSMA/CA and Aloha [7]–[9]. Nevertheless in WBAN environment, these mechanisms are not as effectively as they perform in general wireless networks. Because CSMA/CA and Aloha can not guarantee the transmission delay due to the randomness of the mechanisms, while WBANs have strict delay requirements, e.g. medical-related information. MIMO technology can also be used to deal with coexistence among multiple networks which enables MIMO Interference Cancellation(IC) and Spatial Multiplexing (SM) to enhance network coexistence and performance [10], [11]. However, complex hardware design and high energy consumption hinder its deployment on tiny body sensors. In addition, many other methods [12]–[14] were proposed for general wireless network like WiFi, bluetooth, ZigBee, general sensor networking, and general MANETs to improve the network performance under such coexisting conditions. However, these methods can not be used directly in WBANs as some of these methods assume that the location of each network and the channel conditions between different networks are fixed or changed slowly. Even though MANETS consider the mobility of networks, the movement fashion difference makes it difficult to transplant coexisting methods in MANETS to the area of WBANs.

The newly published standard IEEE 802.15.6 [15], which is specifically designed for WBANs, requires the system to function properly within a $6 \times 6 \times 6$m space when up to 10 WBANs are co-located. In this standard, intra-WBAN interference within a BAN is well addressed by the MAC mechanism. At the same time, three mechanisms to address inter-WBAN interference for multi-WBAN coexistence are also defined, which is channel hopping, beacon shifting and active part interleaving. In more detail, channel hopping method periodically modifies the operating frequency of network for interference mitigation. While in beacon shifting, different coordinators transmit their own beacon frames in different offset times relative to the beginning of the beacon period since beacon frame is important for the whole network. For active part interleaving, the hubs of co-existing WBANs interleave their active parts in beacon period to avoid the possibly concurrent transmission among these WBANs. Even though the standard provides a powerful foundation for coexistence, practical integrated mechanism and detailed procedure for coexistence issue remains blank in the standard. Besides the standard, many methods have been done to address the coexisting problems for WBANs [4], [16], [18], [20]–[27], which contain power control, resource allocation and multi-channel utilization. Even so, a complete integrated mechanism which takes control of coexisting WBANs in every aspect is still needed.

Besides transmission performance issue arisen in multi-WBANs coexistence, QoS-diversity is another important issue that should be seriously considered [16]. Different co-existing WBANs have different communication requirements. For example, in a hospital room, an elder patient with chronic disease need to be monitored in blood pressure, core temperature, oxygen saturation, while another young patient is monitored with capsule endoscope which is related to his illness. The WBAN of elder patient requires only a few bandwidth since the amount of parameters monitored for him is small and the sample rate is low. On the other hand, capsule endoscope deployed in young patient needs much more bandwidth compared with the elder. In addition, when the network resource is insufficient, the WBAN equipped on a human in more critical condition, e.g. patient in intensive care unit, should be set higher priority and firstly allocated the resource to avoid danger when emergency takes place. In summary, QoS-diversity and priority should be taken into consideration when designing mechanism to deal with coexistence of WBANs.

In this paper, an integrated coexisting mechanism called individual distinguish coexisting mechanism is proposed for WBANs. The mechanism can guarantee the transmission performance of each WBAN in multi-WBANs context while provide differentiated shared channel resource for each WBAN depending on its own importance and service requirements. It takes advantages of the coexistence mechanisms in IEEE 802.15.6 standard as the foundation to coordinate the transmission between coexisting WBANs and mitigate the inter-WBANs interference in an distributed and adaptive way without a dedicated center controller among WBANs. Every transmission aspect of coexisting WBANs including co-channel access, shared communication resource allocation, superframe scheduling and transmission power control is considered and specified in this work. The shared communication resource, e.g. transmission time slot, is allocated to each WBAN according to the importance and QoS related parameters. Also, the impact of mobility of WBANs is also considered in the mechanism. The components incorporated in the proposed mechanism can be summarized as follows:

- **Timeslot allocation**: A game-theoretic approach is proposed to deal with timeslot allocation problem among coexisting WBANs in a distributed way. Each WBAN obtains a distinct amount of transmitting timeslot according to its own importance and requirements in the game. Also, the payoff function designed in the game is able to prevent greedy users from requiring much more resource than their demands by adding a punishment in the function.
- **Access control**: An access control method is designed to coordinate coexisting WBANs to access the same channel, which is modified from the beacon shifting mechanism specified in IEEE 802.15.6 standard. Further, channel switching is invoked for the new joining WBAN to find another channel if the current joined channel is fully occupied.
- **Active period scheduling**: Inspired from the active interleaving mechanism proposed in IEEE 802.15.6 standard, we present an active period scheduling method by which active part of each WBAN are interleaved

according to the results in timeslot allocation so as to mitigate the interference caused by the concurrent transmission of co-located WBANs.

- **Power control**: A mobility prediction based power control method is designed to deal with the transmission power of the WBANs in the multi-WBANs context. The method utilizes beacon frame of each WBAN to predict the mobility of each WBAN and the relative distance between a pair of WBANs. Together with the superframe scheduling, the transmission power of each WBAN is decided.

The proposed mechanism is evaluated through simulations where the coexisting scenario is designed as a hospital room. The results demonstrate that the proposed mechanism is stable and convergent in such scenarios and provide differentiated time slots for different WBANs according to their priority conditions. When compared with the original mechanisms specified in IEEE 802.15.6, the transmission performance of the coexisting WBANs under our proposed mechanism is improved in terms of transmission outage probability, transmission energy efficiency, throughput of the networks and transmission delay.

The rest of this paper is organized as follows. Section II consists of related work. In Section III, the system model considered in this paper is described. The game-theoretic based time allocation is presented in detail in Section IV, which is the core of the proposed coexisting mechanism. Section V describes the other three parts of our work and the implementation of our proposed mechanism. Performance evaluations are illustrated in Section VI. Finally, we conclude the paper in Section VII.

II. RELATED WORK

Coexisting is a hot issue of WBANs in recent years. In literature [17], the inter-BAN interference was highlighted as the interference that was generated due to the communications of WBANs in proximity of one another within the same operating frequency. When several nodes in different WBANs try to communicate data in their respective networks at the same time in the same vicinity, interference would increase significantly and therefore reducing the reception probabilities and throughput achieved by all the networks. De Silva *et al.* [18] illustrated that the PDR of the transmission for a WBAN located with several coexisting WBANs would reduce as much as 35%. An experiment was conducted in [19] to examine the transmission performance of WBANS under multi-WBANs situations. The experimental results indicated that the communication under inter-BAN interference will be severely affected without coordination between WBANs. Kim *et al.* [5] conducted experiments in 6 scenarios to investigate the interference effect on the performance of WBANs. The conclusion inferred that it had a possibility to cause a serious problem if inter-BAN interference existed.

Attempting to mitigate inter-WBAN interference, many classes of methods have been studied, which can be summarized as follows:

- Multi-channel technology [4], [18], [20], [21].
- Time slot allocation [16], [22]–[24].
- Power control [24]–[27].

For multi-channel technology, de Silva *et al.* [18] proposed an inter-WBAN interference mitigation system for coexistence issue. The system utilized external sensor nodes which formed a fixed wireless sensor networks to monitor the mobile WBANs and allocate different channels to WBANs that appeared in the areas of those sensor nodes to avoid inter-WBAN interference. However, this method relied on a central controller to coordinate the channel selection. Hence, it was not very suitable for the mobile attribute of WBANs.

Mohamad *et al.* [4] proposed an channel hopping mechanism based on the property of Latin rectangle to retransmit the collided packets so as to address the coexisting WBAN transmission. Kim *et al.* [20] an adaptive channel estimation and selection scheme for coexisting mitigation. The scheme considered channel stability when needing to switch the channel. Moungla and his mates proposed an distributed interference management method to address coexisting among co-channel WBANs [21]. They adopt cognitive radios for proactive interference sensing and channel switching and a flexible Time Division Multiple Access(TDMA) protocol for intra-BAN communication. As stated in [1] and [15] that the number of channels that can be utilized for WBANs is limited, mitigating the inter-BAN interference via multi-channel methods only would lead to the lack of channel resource especially in the dense-deployed areas. Hence, other methods should be incorporated with multi-channel technology to alleviate the critical shortage of channel resource.

In the aspect of time slot allocation methods, RACOON protocol was proposed in [16] to provide QoS control in multiuser scenario for WBANs. The proposed protocol used a dynamic weighted-random-value-comparison scheme to meet priority requirements and a probing-based inter-WBAN interference detection to simplify QoS controls. But a dedicated channel must be occupied by the coordinators of WBANs to negotiate for resource contention. Kim *et al.* [22] proposed a hybrid channel access scheme for coexisting WBANs. In the scheme, contention-free period and contention-based period are interleaved for WBANs according to the coexisting conditions. Ali *et al.* [23] proposed a distributed time reference correlation scheme to allocate time slots to coexisting WBANs. This scheme utilized Walsh Hadamard codes to make orthogonal allocation for different WBANs in order to coordinate inter-BAN interference. However, these methods didn't fully utilize space diversity of coexisting WBANs which resulted in the degradation of total network throughput.

Movassaghi *et al.* [24] proposed an integrated coexistence mechanism which incorporated inter-network channel allocation, channel dynamics prediction and power control. The proposed mechanism was verified to be energy efficient and mitigation-avoiding in channel dynamics coexisting WBANs scenarios. Nevertheless, QoS and priority were not considered in this integrated mechanism.

Power control methods are also used to address coexistence. Lee *et al.* [25] proposed a Qos-aware power control method to coordinate inter-BAN interference. It defined a utility function to indicate QoS satisfaction of each WBANs and used Cucker-Smale model in calculating the appropriate transmission power for coexisting WBANs. However, this method didn't support the mobility of WBANs in coexisting scenarios. Zou *et al.* [26] proposed an Bayesian game based power control method to mitigate the inter-BAN interference. In this power control, different types of links were taken into consideration when calculating power level to reflect the wireless channel diversity in WBAN system. Another game based power control method was proposed in [27] where the authors modeled a non-cooperative game to decide power level for the coexisting WBANs to decrease the interference. The existence and uniqueness of Nash equilibrium were proved in the modeled game and the simulation results demonstrated that the proposed power control method showed effectiveness in multi-WBANs environment. However, QoS diversity and distinguish requirements were not be realized in these two methods.

Game theory has already been proven as an important tools to deal with the coexisting problem in wireless networks due to its distributed manner and convergent attribute. Many game theory methods has been designed in the literatures [8]–[10], [26], [27]. In [8], game theory was used to model and analyze the IEEE 802.11 DCF mechanism. Babaei *et al.* [9] modeled the contention access transmission as a non-cooperative game and the actions of each player (node) were the access probability. The payoff functions in both literatures were designed as the throughput of each node. They aimed to find the Nash equilibrium and improve the total network throughput. A novel two-round game framework was proposed in [10] to optimize the performance of coexisting networks equipped with MIMO. In the game model, two network strategies in equilibrium and the corresponding closed-form utilities were designed.

In the area of WBANs, two power control game were proposed in [26] and [27]. In both literatures, the authors modeled each coexisting WBAN as a player and actions of each player were transmission power levels. Both payoff functions were designed as the difference between the network utility and priced power.

In addition, channel characterization of WBANs plays an important role in the research works of WBANs coexisting as precise channel mode is utmost prerequisite for the development of reliable communication system. Many experiments and measurement campaigns have been conducted to characterize different kinds of wireless channels of WBANs [28]–[38].

Specifically, on-body wireless channels were studied and modeled in the literature [28]–[32]. Herein, Forrister *et al.* [28] measured on-body channel based on 7 human subjects performing 7 activities with 3 different narrowband antenna frequencies and 3 different antenna configurations. In [29], on-body channels were characterized by means of experiments on a human head where a pair of differential electrodes is applied to simulate the on-body communications. An Ultra Wide Band(UWB) on-body channel characterization was presented in [30]. The characterization addressed the influence of medium presence on the reflection loss of horn and textile antennas. Another UWB on-body channel characterization was conducted in [31] where the parameters of path loss model are statistically determined by analyzing measurement data and both the Line-of-Sight(LOS) and None-Line-of-Sight(NLOS) channel conditions are considered in the measurement. In [32], Both on-body and body-to-body channels were characterized using the $k-\mu$ fading model.

Body-to-body channels were measured and concluded in [32]–[35]. Mani *et al.* [33] utilized three on-body antenna positions and multiple human mobility scenarios to investigate the body-to-body channel variations. A comprehensive channel model was also derived depending on the mutual body position in terms of distance and orientation. Another body-to-body channel measurement was conducted in [34]. In this measurement, not only different body motion scenarios and on-body antenna placements were considered, but also both indoor and outdoor environments were taken into account. In [35], a Lognormal mixture shadowing model was used to model the body-to-body channels in running and cycling activities.

As an alternative communication scheme for WBANs, Human Body Communication(HBC), which uses human bodies as the communication medium to provide better communication performance, has also been investigated [36]–[38]. In [36], an extended HBC channel model was established based on the measured channel responses which were obtained from the test fixtures in the human arm. Zhang *et al.* [37] measured and characterized a capacitive HBC channel considering different electrode positions and different body shapes. Based on the measurement results, a HBC channel model was derived and the model parameters were extracted by fitting methods. In [38], HBC channels were measured in terms of Signal-to-Noise-Ratio(SNR) based on impulse radio technology. The results of the behavior of SNR showed how signals will propagate through the human body communication channel.

III. SYSTEM ARCHITECTURE

In this section, WBAN architecture and coexistence scenario are introduced first. Channel models including on-body channel and body-to-body channel are described following. The transmission and reception models are presented at the end of this section.

A. COEXISTENCE SCENARIO DESCRIPTION

We consider a coexistence scenario where N WBANs are co-located in a hospital room with size $6m \times 6m$. Each WBAN consists of one coordinator and several sensor nodes. The coordinator is deployed at the front side of abdomen since the location is relatively stable on the human body.

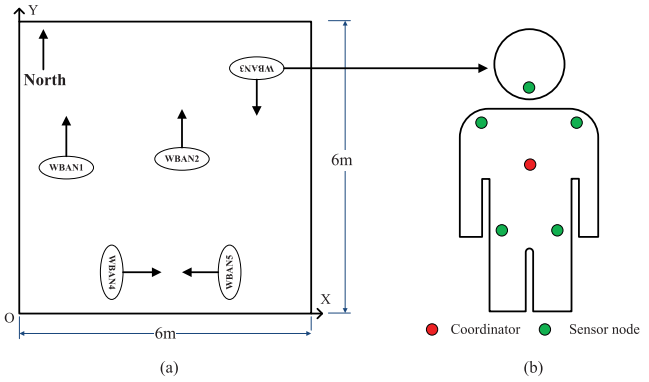

FIGURE 1. An example of Coexistence scenario. (a) Coexistence scenario. (b) WBAN architecture.

Sensor nodes are distributed around the coordinator on the different location of the human body. An example of the coexistence scenario is illustrated in Fig. 1. The intra-WBAN communications are arranged via beacon-enabled superframe MAC specified in IEEE 802.15.6 [15] where TDMA is adopted for sensor nodes to access the channel for reporting the sensed information to the coordinator. Therefore, no intra-BAN interference appears within each WBAN [39]. In this paper, we assume that the coordinator of each WBAN has the ability to synchronize with each other.

Each WBAN moves randomly in the room space. We assume that the moving of each WBAN takes place at the beginning of a beacon period and remains the state during the period. Each WBAN randomly selects to move forward, stand still or change moving direction with the possibilities of p_{mf}, p_{ss} and p_{cmd}, respectively. The speed of each WBAN is set to be v_{wban} and the moving direction consists of north, south, west and east as shown in Fig. 1. When a WBAN reaches the room edge or two WBANs crash into each other, the moving direction reverses.

B. CHANNEL MODEL

We adopt the Free Space Path Loss (FSPL) model to obtain the path loss for inter-BAN channels based on the distance between the transmitter and the receiver. For the intra-BAN channels, we adopt the path loss model designed in Castalia simulator [40], which is a modified version of FSPL according to the modeling experiments and on-body channel measurements. In a word, the path loss model for intra-BAN and inter-BAN channel can be summarized as follows:

$$PL(d) = PL_0 + 10 \cdot n \cdot log_{10}(\frac{d}{d_0}) + S. \quad (1)$$

where PL_0 is the pathloss at reference distance d_0, n is the pathloss exponent, d is the transmission distance between the sender and the receiver and S is the shadowing component. In particular, n is set to 2 for the inter-BAN channel as the inter-BAN communications take place in free space [6], [21], [24] and set to 2.4 for intra-BAN channel since intra-BAN communications suffer from body surface absorption and attenuation [5], [40]. For intra-BAN pathloss, S is a postural shadowing component which is a gaussian zero-mean random variable with standard deviation σ. When it comes to inter-BAN channel, according to the shadowing effect measurement in [41], the path loss would increase more than 15dB when the path is obstructed. Hence, S is set to 15dB if the transmission path is NLOS obstructed by human body. Otherwise, if the transmission path is LOS, S is 0dB. The detailed representation for LOS/NLOS conditions and graphical examples are illustrated in Table I and Fig. 2, respectively, to explain the shadowing effect and LOS/NLOS path in channel model. In the table, V_1 and V_2 represent the moving directions of WBAN1 and WBAN2, respectively, while $X_{1(2)}$ and $Y_{1(2)}$ represent the coordinate of WBAN1(2) on the X axis and Y axis as shown in Fig. 2, respectively.

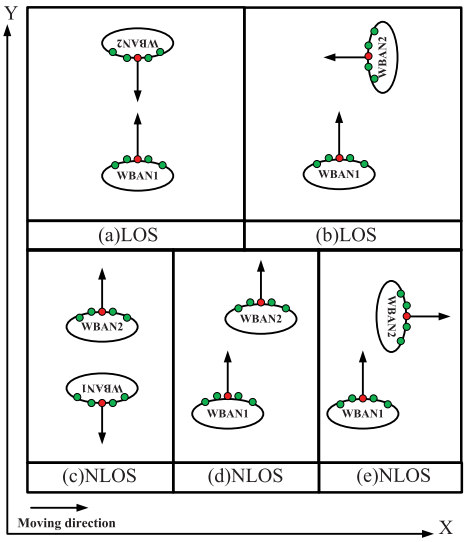

FIGURE 2. Shadowing effect on inter-BAN channel.

TABLE 1. LOS/NLOS conditions in relation with moving directions and locations.

Channel conditions	Moving direction	Coordinate
LOS(a)	$V_1 = West, V_2 = East$	$X_1 > X_2$
	$V_1 = North, V_2 = South$	$Y_1 < Y_2$
LOS(b)	$V_1 = East, V_2 = South$	$X_1 < X_2, Y_1 < Y_2$
	$V_1 = West, V_2 = South$	$X_1 > X_2, Y_1 < Y_2$
	$V_1 = West, V_2 = North$	$X_1 > X_2, Y_1 > Y_2$
	$V_1 = East, V_2 = North$	$X_1 < X_2, Y_1 > Y_2$
NLOS(c,d,e)	Otherwise	

Note: For simplicity of the condition description, we only present half of LOS conditions. The other half can be derived via the exchange of the subscript 1 and 2 in each condition.

C. TRANSMISSION AND RECEPTION MODEL

In this paper, a packet will be correctly received if two conditions are satisfied : (1)Signal-to-Interference-plus-Noise-Ratio (SINR) is higher than a threshold T_{SINR}, (2)Received Signal Strength Indicator (RSSI) is higher than receiving sensitivity, $Rx\_sensitivity$ of the receiver. Herein, SINR of the

received packets within n_{th} WBAN is determined in Eq. (2)

$$SINR_n = \frac{p_n \times h_{nn}}{\sum_{j=1,j\neq n}^{N} h_{jn} \times p_j + N_0} \tag{2}$$

where p_n stands for the transmitting power of the transmitter in n_{th} WBAN, p_j the transmitting power of the transmitter in j_{th} WBAN which transmits concurrently with nth WBAN, h_{nn} for the channel gain of the n_{th} intra-BAN channel and h_{jn} for the channel gain of the inter-BAN channel between j_{th} WBAN and n_{th} WBAN. That is to say, $\sum_{j=1,j\neq n}^{N} h_{jn} \times p_j$ stands for the inter-BAN interference to the n_{th} WBAN. N_0 stands for the background noise received by the receiver. On the other hand, RSSI of a packet is determined in Eq. (3)

$$RSSI = Tx\_power - pathloss \tag{3}$$

where Tx_power stands for the transmitting power of the packet and $pathloss$ for the path loss of the transmitting channel which is described in Section III-B (Note that channel gain in Eq. (2) is the negative value of path loss for the corresponding channel).

IV. A GAME FOR TIMESLOT ALLOCATION

As presented in Section I, the proposed coexisting mechanism consists of four parts. More specific, the game-theoretic based timeslot allocation is the core of the mechanism, while the other three parts assist timeslot allocation to achieve the coexistence of co-located WBANs. Hence, we exclusively designate this section to present the game in the proposed coexisting mechanism, verify the existence and uniqueness of the Nash equilibrium and develop a distributed algorithm for each player in the game to converge to the point of Nash equilibrium.

As mentioned in Section II, the reason why we utilize game theory to address the time slot allocation in our coexisting mechanism is due to the advantages of game theory that it has the distributed manner and possible convergent result (Nash equilibrium) which perfectly matches the design requirements of coexisting mechanism for WBANs. Also, in consideration of different network priorities and prevention of greedy WBAN users, we design a novel payoff function in the game to fulfil the differentiated timeslot allocation according to the priorities of each WBAN.

A. GAME FORMULATION

We formulate the problem of timeslot allocation for co-located WBANs as a non-cooperative game in which each coexisting WBAN acts as a player and announces its timeslot demanded for the upcoming beacon period. The payoff of each WBAN is a utility function that describes the value of the demanding timeslots. Each WBAN attempts to maximize its utility function selfishly.

We formally define the game as a triple $G = \{N, (D_i)_{i\in N}, (U_i)_{i\in N}\}$, where $N = \{1, \ldots, N\}$ is the finite set of players, D_i is the available strategies and U_i is the utility function to evaluate the payoff. In our formulation, players are coexisting WBANs and the number of demanding timeslots is the strategy that players adopt. Assuming that there is totally T_{total} available slots in one beacon period, the strategy set is defined as $D_i = \{0, 1, \ldots, T_{total}\}$. The utility function in the game is designed in Eq. (4):

$$U_i(D_i, D_{-i}) = a_i \cdot T_{total} \cdot \frac{D_i}{\sum_{j=1}^{N} D_j} - c \cdot D_i \tag{4}$$

where a_i is a parameter related to the priority and requirements which is decided by individual conditions like disease severity, service level, etc.. c is the unified payment of the demand for time slots which is used to prevent greedy users from requiring much more resource than their demands. In this paper, the value of a_i should set to be larger than c. Each player chooses a strategy in strategy set so as to maximize the value decided in Eq. (4).

B. NASH EQUILIBRIUM IN THE GAME

Next, we discuss the Nash Equilibrium in the formulated game which is the most important strategy profile in the game. As we know, players are selfish and always try to maximum their own utility function values by selecting the best response strategy, given as:

$$b_i = \underset{D_i}{arg\ max}\ U_i(D_i, D_{-i}) \tag{5}$$

i.e., the value of D_i maximizes U_i with a fixed D_{-i} which is all the other players's selecting strategies. A strategy profile $\widetilde{D} = \{D_i, D_{-i}\}$ is a Nash Equilibrium if, for each $i = 1, \ldots, N$, $D_i = b_i$ holds.

Theorem 1: There exists a unique Nash equilibrium in the time allocation game defined in Section IV-A.

Proof: As can be seen in Eq. (4), the utility function $U_i(D_i, D_{-i})$ is continuous within the strategy range $[0, T_{total}]$. For each player i, we assume that D_{-i} is fixed and take the derivation of $U_i(D_i, D_{-i})$ with respect to D_i as below:

$$\frac{\partial U_i}{\partial D_i} = a_i \cdot T_{total} \cdot \frac{\sum_{j=1,j\neq i}^{N} D_j}{(\sum_{j=1,j\neq i}^{N} D_j + D_i)^2} - c \tag{6}$$

Then, by taking second derivation of U_i with respect to D_i, we obtain:

$$\frac{\partial^2 U_i}{\partial (D_i)^2} = -2a_i \cdot T_{total} \cdot \frac{\sum_{j=1,j\neq i}^{N} D_j}{(\sum_{j=1,j\neq i}^{N} D_j + D_i)^3} \tag{7}$$

Since $\sum_{j=1,j\neq i}^{N} D_j + D_i > 0$, it is obvious that $\frac{\partial^2 U_i}{\partial (D_i)^2} < 0$. As a result, the utility function $U_i(D_i, D_{-i})$ is a strictly concave

with respect to D_i. On the other hand, as the strategy set of each player is $D_i = [0, T_{total}]$, the global strategy profile of the game, given by the Cartesian product of all players strategy, i.e. $D_1 \times D_2 \times \ldots \times D_N$, is a non-empty, convex and compact subset of Euclidian space. According to theorem 1.2 in *Game Theory* [42], if the non-cooperative game has non-empty compact convex subsets of a Euclidean space, and the payoff functions of players are continuous in the domain of strategy set and quasi-concave with respect to corresponding strategy variables, there exists a unique Nash equilibrium in the game. As $U_i(D_i, D_{-i})$ is concave with respect to D_i, it is also a quasi-concave function. In conclude, the proposed game in Section IV-A has a unique Nash equilibrium.

C. A DISTRIBUTED ALGORITHM TO NASH EQUILIBRIUM

As shown in the previous subsection, the point of Nash equilibrium is a strategy profile where each player in the game select the best response strategy corresponding to the strategies of the other players. According to Eq. (5) and the derivation that $U_i(D_i, D_{-i})$ is strictly concave, we can obtain the best response point b_i of each player by setting Eq. (6) to 0.

$$a_i \cdot T_{total} \cdot \frac{\sum_{j=1,j\neq i}^{N} D_j}{(\sum_{j=1,j\neq i}^{N} D_j + D_i)^2} - c = 0 \tag{8}$$

After mathematical derivation, we get

$$b_i = \sqrt{\frac{a_i \cdot T_{total} \cdot \sum_{j=1,j\neq i}^{N} D_j}{c}} - \sum_{j=1,j\neq i}^{N} D_j \tag{9}$$

Denoting $R_{-i} = \sum_{j=1,j\neq i}^{N} D_j$, b_i can be obtained in Eq. (10):

$$b_i = \sqrt{\frac{a_i \cdot T_{total} \cdot R_{-i}}{c}} - R_{-i} \tag{10}$$

Theorem 2: The unique Nash equilibrium in the proposed game is $\widetilde{D} = \{b_1, b_2, \ldots, b_N\}$ where each b_i is calculated by Eq. (10), if and only if $\frac{a_1-c}{a_1} + \frac{a_2-c}{a_2} + \cdots + \frac{a_N-c}{a_N} = 1$

Proof: Assuming that $b_1 + b_2 + \cdots + b_N = T_{total}$, i.e. the sum of each player's best response strategy is equal to the total number of available timeslots. Eq. (8) can be further derived as:

$$\begin{aligned} a_i \cdot T_{total} \cdot \frac{R_{-i}}{(R_{-i} + D_i)^2} - c &= 0 \\ a_i \cdot T_{total} \cdot \frac{R_{-i}}{(R_{-i} + D_i)^2} &= c \\ a_i \cdot T_{total} \cdot \frac{T_{total} - D_i}{(T_{total})^2} &= c \\ a_i \cdot \frac{T_{total} - D_i}{T_{total}} &= c \end{aligned}$$

Algorithm 1 The Distributed Algorithm to Nash Equilibrium

1: **Input**: a_i, c and T_{total}.
2: **Initialization**:
3: Set a_i and $D_i(0) = T_{total}/N$.
4: **In each iteration (n)**:
5: *Require:* $D_i(n-1), i = 1, \ldots, N$.
6: $D_i(n) = \sqrt{\frac{a_i \cdot T_{total} \cdot \sum_{j=1,j\neq i}^{N} D_j(n-1)}{c}} - \sum_{j=1,j\neq i}^{N} D_j(n-1)$
7: **Output**: $D_i(n)$.

We can obtain b_i in Eq. (11):

$$b_i = \frac{a_i - c}{a_i} \cdot T_{total} \tag{11}$$

Hence, according to the assumption that $b_1 + b_2 + \cdots + b_N = T_{total}$

$$\frac{a_1 - c}{a_1} \cdot T_{total} + \frac{a_2 - c}{a_2} \cdot T_{total} \cdots + \frac{a_N - c}{a_N} \cdot T_{total} = T_{total} \tag{12}$$

Dividing each side of Eq. (12) by T_{total}:

$$\frac{a_1 - c}{a_1} + \frac{a_2 - c}{a_2} + \cdots + \frac{a_N - c}{a_N} = 1 \tag{13}$$

Since strategy profile $\widetilde{D} = \{b_1, b_2, \ldots, b_N\}$ consists of best response strategy of each players, $\widetilde{D}$ is the Nash equilibrium of the game. According to **Theorem 1**, when $\frac{a_1-c}{a_1} + \frac{a_2-c}{a_2} + \cdots + \frac{a_N-c}{a_N} = 1$, $\widetilde{D}$ can be obtained from Eq. (10), which is the unique Nash equilibrium in the proposed game.

According to the definition of Nash equilibrium, when all players select best response given other players's strategy, the game reaches the equilibrium. Taking this definition and **Theorem 2** as basis, we develop a distributed iterative algorithm for each player i, $i = 1, \ldots, N$ to converge at the point of Nash equilibrium. The detailed algorithm can be seen in Algorithm 1. It should be noted that in the algorithm we assume $\frac{a_1-c}{a_1} + \frac{a_2-c}{a_2} + \cdots + \frac{a_N-c}{a_N} = 1$ to guarantee the existence of Nash equilibrium. In each iteration of Algorithm 1, each player calculates its best response strategy based on the strategy that other players selected in the previous iteration, and selects the best response as its strategy for the current iteration. The method in algorithm 1 to select strategy is also called Picard iteration method [26].

According to the [43, Th. 2.1], Picard iteration will converge to the Nash Equilibrium of the proposed game. Since there is only one Nash equilibrium in the proposed game, each player will finally converge to the unique Nash equilibrium point after several iterations.

V. THE PROPOSED COEXISTING MECHANISM

In this section, the detailed coexisting mechanism will be illustrated based on the theorems and algorithm derived in Section IV. A diagram of coexisting mechanism which contains the relationship between each part of the proposal is shown in Fig. 3.

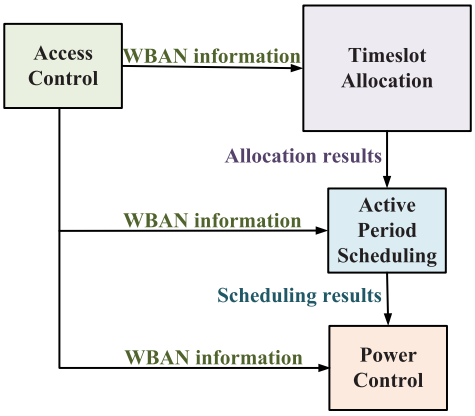

FIGURE 3. The diagram of the proposed coexisting mechanism.

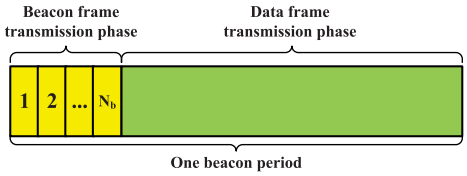

FIGURE 4. Beacon period structure of the mechanism.

A. ACCESS CONTROL

Access control takes charges of the transmission of beacon frame for each coexisting WBAN in the same channel and admission process for the new joining WBAN. It is designed upon the beacon shifting mechanism in IEEE 802.15.6. Only a small modification to IEEE 802.15.6 specification is needed to fulfill the proposed access control.

A beacon period structure of the proposed coexisting mechanism is shown in Fig. 4. The period is divided into two phases which are beacon frame transmission phase and data frame transmission phase, the length of which are both fixed. The beacon frame transmission phase located at the beginning of every beacon period contains N_b slots and each slot allows to transmit one beacon frame of a certain coexisting WBAN. While data frame transmission phase is used for intra-BAN data communications of each WBAN.

At the beginning of every beacon period, each coexisting WBAN broadcasts its beacon frame with maximum power to the sensor nodes within its network and also to other co-located WBANs in its dedicated beacon transmission slot. The beacon frame contains its differentiated priority and requirements based parameter a, start time and end time of its active period in this beacon period, intra-BAN communication information for the active part and time slot demand for the next beacon period. Since the coordinator is usually a mobile phone or a PDA which is hard-ware developed device, we assume that beacon frames are always successfully received among coexisting WBANs.

When a WBAN switches to a new operating channel or enter a new room, it listens to the beacon frame transmission phase in its first listened beacon period and check how many WBANs are there in the same channel and same room.[1] If there is no idle slot, the new WBAN switches to another channel. Otherwise, in the second beacon period, it randomly select a idle beacon transmission slot to broadcast its beacon frame to announce participation. If two or more new joining WBANs collide at the beacon transmission phase, they will randomly select transmission slot again. When beacon frame of a certain new WBAN is transmitted T_{max} times and still collides with other beacon frames, it switches to another channel. When the beacon frame of a new WBAN is successfully broadcasted, the slot it uses becomes its dedicated beacon frame transmission slot.

Algorithm 2 Parameter Revision Algorithm

1: **Input**: $a_i, i = 1, \ldots, N$ and c
2: **for** each $i \in [1, N]$ **do**
3: $\hat{a} = \frac{c}{1-\frac{\frac{a_i-c}{a_i}}{\sum_{i=1}^{N}\frac{a_i-c}{a_i}}}$
4: **Output**: $\hat{a}$.
5: **end for**

According to **Theorem 2**, when new WBANs have successfully broadcasted their beacon frames or WBANs have leaved through switching their operating channel/leaving the room, the parameter a of each coexisting WBAN needs to be revised to satisfy $\sum_{i=1}^{N}\frac{a_i-c}{a_i} = 1$. The revision for each coexisting WBAN is presented in Algorithm 2. In the algorithm, N stands for the total number of coexisting WBANs and $\hat{a}$ is the revised parameter to be used in time slot allocation game. Then, the calculated $\hat{a}_i$ is adopted by each WBAN in Algorithm 1.

B. ACTIVE PERIOD SCHEDULING

The active period scheduling is designed inspired from the active part interleaving mechanism specified in IEEE 802.15.6, the main idea of which is to allocate orthogonal active period to each coexisting WBAN in one superframe so that there is only one active WBAN can transmit at one time. Different from the original mechanism in the standard, the proposed active period scheduling allows more than one coexisting WBAN to concurrently make their communications in order to increase the throughput in one beacon period.

We denote θ as space reuse factor, which means the number of coexisting WBANs transmitting concurrently at one time in the data frame transmission phase. Assuming that data frame transmission phase in one beacon period contains T time slots, there are actually θT available slots for coexisting WBANs to communicate. The steps of active period scheduling are organized as follows:

Step 1 θT slots in total are arranged in a line and divided into groups with the fixed length of T slots(If θ is not

[1]The WBANs too far away or in another room is not considered as coexisting WBAN since the path loss is so large that the beacon frame can not be heard and interference can be negligible due to the large distance or wall obstruction of the room

a integer, the last group does not has the full length of T. For example, if θ is 2.5, the last group has the length of $0.5T$.).

Step 2 Based on the timeslot allocation results and the sequence of beacon frame transmission in the beacon frame transmission phase, the time slots will be allocated to the WBAN in the sequence manner as they broadcast their beacon frames. The number of scheduled slots depends on the allocation results.

Step 3 The location of each slot in its group is the actual slot location in the data frame transmission phase. For example, WBAN A is allocated with the $1st$ slot in group 1 while WBAN B is allocated with the $1st$ slot in group 2. Then, WBAN A and WBAN B will both transmit in the $1st$ slot of data frame transmission phase.

To better illustrate the active period scheduling, an example is shown in Fig. 5. In this example, there are four coexisting WBANs, which are WBAN A, WBAN B, WBAN C and WBAN D, respectively. Data frame transmission phase in one superframe has 20 time slots and θ is set to 2. Hence, there are totally $20 \times 2 = 40$ timeslot resource that can be allocated to coexisting WBANs. Also, as can be seen in the figure, the beacon frame transmission sequence during beacon frame transmission phase is :1)WBAN A, 2)WBAN B, 3)WBAN C, 4)WBAN D. The timeslot allocation results shown in the figure indicate that WBAN A has 15 timeslots to transmit in the data frame transmission phase of this scheduling superframe. In the same way, B, C and D has 10, 9 and 6 timeslots, respectively. Then, the active period scheduling will be implemented in the following steps:

Step 1 40 timeslots are arranged in a line and divided into 2 groups with fixed length of 20 timeslots(Group 1 and Group 2).

Step 2 WBAN A is allocated with the first 15 timeslots in Group 1 as it transmits beacon frame at the first place in beacon frame transmission phase. In the same way, WBAN B is allocated next with 10 timeslots. Since Group 1 as only 5 timeslots left, the first 5 timeslots of Group 2 are sequentially allocated to WBAN B. Then, WBAN C is allocated with the following 9 timeslots. The last 6 timeslots are finally allocated to WBAN D.

Step 3 Based on Step 2, the final active period scheduling results can be found in Fig. 5(b). The active period of WBAN A is $1st - 15th$ timeslot. While the active period of WBAN B is $1st - 5th$ and $16th - 20th$ timeslot as WBAN B is allocated $16th - 20th$ timeslot in Group 1 and $1st - 5th$ timeslot in Group 2. The active periods of WBAN C and WBAN D are $6th - 14th$ and $15th - 20th$ timeslot, respectively.

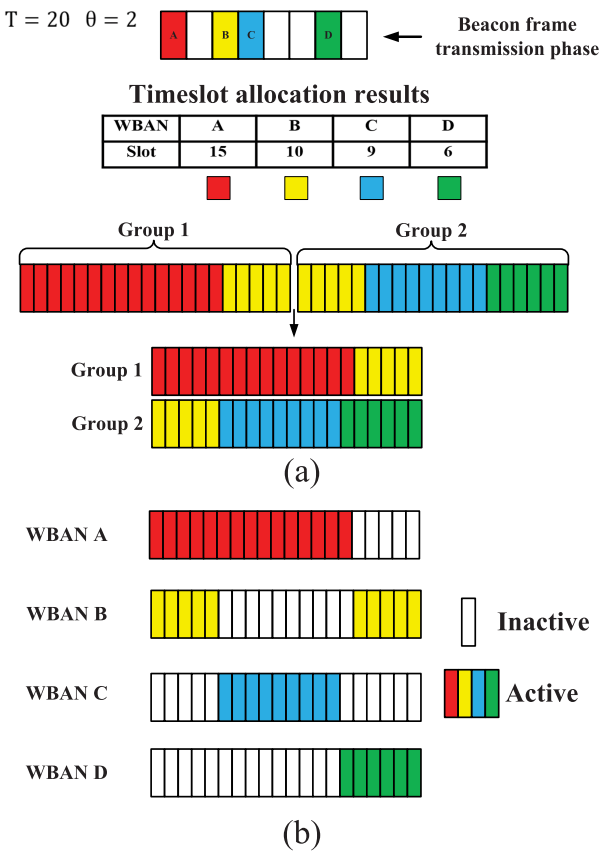

FIGURE 5. An example of active period scheduling.(a)Active period scheduling (b)Active period of each coexisting WBAN in one beacon period.

C. POWER CONTROL

As described in Section V-A, beacon frames are broadcasted and received among coexisting WBANs. Besides, after the active period scheduling, each WBAN knows exactly that in each timeslot of the following beacon period, which WBANs will concurrently transmit. Hence, we utilize the reception conditions of each beacon frame and the active period scheduling results to indicate the power control for each WBAN. In detail, the RSSI derivation between two adjacent beacon periods are used to predict the mobility of concurrently transmitting WBANs and indicate the transmitting power within WBANs in each time slot of the next period according to the active period scheduling results.

We denote $\Delta_{ij}(n)$ as the RSSI derivation of the beacon frame from ith WBAN to jth WBAN between $(n-1)th$ and nth beacon period which can be expressed as:

$$\Delta_{ij}(n) = RSSI_{ij}(n) - RSSI_{ij}(n-1) \tag{14}$$

where $RSSI_{ij}(n)$ represents the RSSI value of beacon frame that is transmitted by ith WBAN and received by jth WBAN. Since WBANs are dynamic and the movements of each WBANs are hard to be precisely predicted, we make use of the derivation to predict the relative position for each pair of coexisting WBANs so as to decide the transmitting power within each WBAN. The predication of the relative position for one pair of WBANs is listed in Table 2. It can be obviously indicated that when $\Delta > 0$ this pair of coexisting WBANs are getting closer and we can roughly predict that they may still

TABLE 2. Prediction principle.

Δ	> 0	$= 0$	< 0
Relative position	Closer	Unchanged	Further

get closer in the next beacon period with a large possibility. In the same way, we can make prediction upon the condition $\Delta < 0$. When $\Delta = 0$, it is not certain whether two WBANs are going to move towards, leave inversely or just stand still. In this condition, we just regard the relative position of this pair unchanged.

Based on the relative position predication, the power control algorithm to each coexisting WBAN $i, i = 1, \ldots, N$ in a certain time slot x is shown in Algorithm 3 (All the values appear in the algorithm is in unit of dB). In the algorithm 3, P_U and P_D stand for the maximum and minimum transmitting power allowed for WBANs. N_0 is the background noise power, which can be measured in the certain application scenario, and we can adopt the averaged value of background power as N_0. Ω_i^x is the set of WBANs that concurrently transmit with WBAN i at slot x. Δ_i is the set of $\Delta_{ji}(n), j = 1, \ldots, N, j \neq i$. While *RSSI* represents the set of RSSI values of data frames from sensor nodes within WBAN i ($RSSI_i^{intra}$) and RSSI values of beacon frames from all other coexisting WBANs. It can be seen from line 9-10 that $\Delta > 0$ indicates that the corresponding pair of WBANs will get closer in the near future. Hence, when deciding the power for the following transmission, pathloss between the corresponding pair is decreased by Δ to show impact of WBAN movements. When $\Delta = 0$, we predict that the relative position of two WBANs remain unchanged. As a result, we only add a small value (*margin*) to the path loss for reliable transmission (line 11-12). When $\Delta < 0$ which indicates the relative position becomes further, the pathloss should be increased due to the future movement. However, in order to guarantee the small amount of inter-BAN interference, we remain the corresponding pathloss unchanged.

Algorithm 3 Power Control

1: **Input** $P_U, P_D, T_{SINR}, margin, N_0$.
2: **Initialization**:
3: Set $Tx\_power_i(0) = P_U$
4: **In the beacon period(n)**:
5: *require*: $\Omega_i^x, Tx\_power_i(n-1), \Delta_i(n), RSSI$.
6: $RSSi_{min} = min(RSSI_i^{intra})$
7: $PL_i = Tx\_power_i(n-1) - RSSI_{min}$
8: **for** each $j \in \Omega_i^x$ **do**
9: **if** $\Delta_{ji}(n) > 0$ **then**
10: $PL_{ji} = P_U - RSSI_{ji}(n-1) - \Delta_{ji}$
11: **else if** $\Delta_{ji}(n) = 0$ **then**
12: $PL_{ji} = P_U - (RSSI_{ji}(n-1) + margin)$
13: **else**
14: $PL_{ji} = P_U - (RSSI_{ji}(n-1)$
15: **end if**
16: **end for**
17: $t = 10log(\frac{10^{T_{SINR}/10} \cdot (\sum_{j \in \Omega_i^x} (10^{P_U/10} \cdot 10^{(-PL_{ji}/10)}) + 10^{N_0/10})}{10^{(-PL_i/10)}})$
18: $Tx\_power_i(n) = max(RSSI_{min} + Rx\_sensitivity, t)$
19: **if** $Tx\_power_i(n) > P_U$ **then**
20: $Tx\_power_i(n) = P_U$
21: **end if**
22: **if** $Tx\_power_i(n) < P_D$ **then**
23: $Tx\_power_i(n) = P_D$
24: **end if**
25: **Output**: $Tx\_power_i(n)$.

D. IMPLEMENTATION

In this part, we will illustrate how the four parts of the proposed mechanism are integrated and implemented on coexisting WBANs. Also, we will discuss the advantages of the proposed coexisting mechanism.

The four parts of coexisting mechanism are all executed in the coordinator of each WBAN since it is more powerful. A diagram of integrated implementation is shown in Fig. 6. As mentioned in Section V-A, beacon frame broadcasted by a certain WBAN contains its differentiated parameter a and time slot demand for the next beacon period. It also contains the information to indicate the intra-BAN communication in this data frame transmission phase.

After receiving all the beacon frames transmitted in the beacon frame transmission phase, each WBAN obtains all the values of a and the demand of time slot for the next beacon period. Hence, each WBAN is able to know whether coexisting WBANs change or not. If changing happening, the parameter revision will takes place as shown in Algorithm 2. Next, depending on the collected demands of each WBAN, time slots are allocated to each WBAN in proportion as follows in Eq. (15):

$$S_i = min(\frac{D_i}{\sum_{n=1}^{N} D_n}, T) \tag{15}$$

where S_i is the actual total number of time slots allocated for *ith* WBAN. At meantime, each WBAN calculates its demand of slots for the next beacon periods with $\hat{a}$ and $D_i, i = 1, \ldots, N$. It should be emphasized that the one iteration in Algorithm 1 is indeed one beacon period in implementation. Since demand of each WBAN is known to all, each WBAN obtain $S_i, i = 1, \ldots N$. Then, based on S_i and the sequence in beacon frame transmission period, active period scheduling is finished by each WBAN. As a result, Ω in algorithm 3 can be obtained.

On the other hand, when receiving beacon frames, each WBAN records the RSSI values of beacon frame from other coexisting WBAN and calculates RSSI derivation Δ of each WBAN. At the end of active period of each WBAN, the coordinator also acquires the RSSI values of data frames from its sensor nodes. Then, according to Ω, Δ and acquired RSSI values, power control can be done for each time slot in the active period according to Algorithm 3. In addition

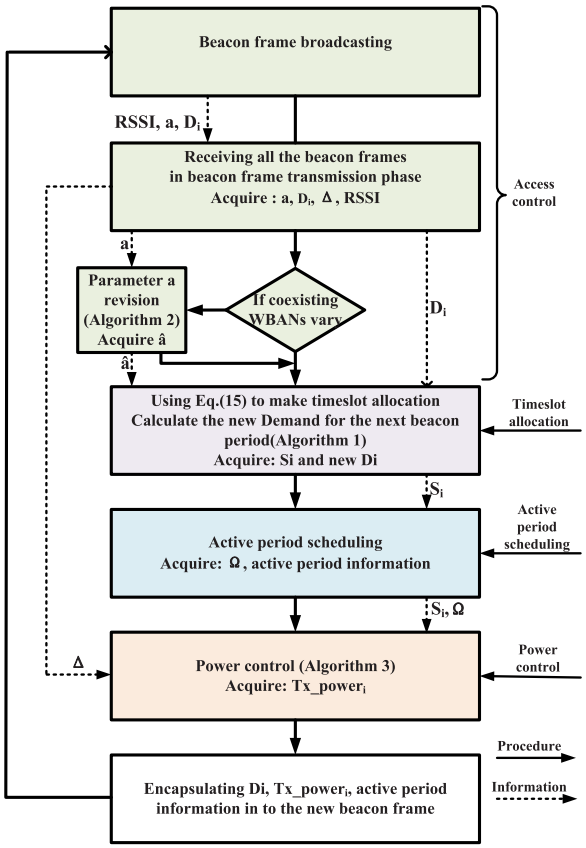

FIGURE 6. The diagram of the coexisting mechanism.

to the description of implementation, the **initialization** in Algorithm 1 and 3 are invoked only when a WBAN joins a new coexisting network.

At last, time slot demand, active period information and intra-BAN communication information including transmitting power and intra-BAN scheduling are loaded in the beacon frame and broadcasted at the dedicated transmission slot in the next beacon period.

In conclusion to this section, we organize the advantages of our proposed individual distinguish coexisting mechanism as below:

- The proposed mechanism is an integrated mechanism to deal with coexisting problem based on the methods recommended in IEEE 802.15.6.
- The proposed mechanism is a distributed mechanism which is executed adaptively by every coexisting WBAN to cooperate the communication and mitigate the inter-BAN communication. It is adaptive to the variation of the coexisting WBAN condition.
- The proposed mechanism is able to make differentiated resource allocation to each involved WBAN based on its attributes related to the service requirement and priority. When abnormal condition happens, the whole coexisting system is able to recover to the equilibrium quickly via convergent algorithm.

TABLE 3. The typical transmission power consumption of the CC2420.

Power Level	Output(dBm)	Power(mW)
3	-25	29.04
7	-15	32.67
11	-10	36.3
19	-5	46.2
31	0	57.42

- To deal with the moving nature of WBANs, the power control in the mechanism makes use of beacon frames to predict the mobility so that the transmission reliability can be guaranteed.
- The proposed mechanism is compatible with IEEE 802.15.6 specification with only a little modifications on the beacon transmission which can be easily realized.

VI. PERFORMANCE EVALUATION

In this section, the performance of the proposed coexisting mechanism is evaluated in the scenario described in Section III via simulations.

A. SIMULATION SETUP

The simulation is designed on Matlab platform. The coexisting scenario described in Section III-A is used to evaluate the performance of the proposed mechanism. Channel model and transmission model described in Section III-B and III-C are also adopted in the simulation.

In order to examine the energy consumption performance, we use the energy depletion parameter of CC2420 radio chip [44] in the simulations which is taken from Castalia simulator and is widely adopted in WBANs related researches. The CC2420 radio chip provide 31 different transmission power levels from -25 dBm to 0dBm. The typical transmission power levels consumption parameters are listed in Table 3. It should be noted that the selection of CC2402 transceiver is to conveniently illustrate the energy efficiency in the simulation due to its clear relationship between transmission power and the corresponding energy consumption. In reality, the transceiver used in WBANs may be more efficient in terms of energy depletion.

Other parameters in the simulation are listed in Table 4. The length of beacon period is set to be $8 \times 10 + 30 \times 5 = 230ms$ in order to satisfy delay requirements of medical applications [1]. It is also assumed that in one slot only one data frame can be transmitted within a WBAN.

B. PERFORMANCE EVALUATION

In this part, the performance of the proposed mechanism is evaluated and analyzed via simulation results.

First of all, the convergence property of the timeslot allocation game is validated and the performance of the corresponding algorithm is analyzed. Fig. 7 shows the number of allocated time slots to each WBAN with different values of a via algorithm 1 and Eq. (15). The spatial reuse factor θ is set to 2. It can be seen from the figure that WBANs in

TABLE 4. Simulation parameters.

Parameter	Value
Room size	6m×6m
N	5
p_{mf}	0.6
p_{ss}	0.3
p_{cmd}	0.1
v_{wban}	0.5m/s
PL_0	55dB
d_0	1m
σ	4
Rx_sensitivity	-88dBm
N_0	-95dBm
c	1
T	30
T_b	8
Data frame slot duration	5ms
Beacon frame slot duration	10ms
Maximum delay	500ms
Simulation times	10000s
The number of sensor nodes in a WBAN	5
T_{max}	3
margin	0.5dB
P_U	0dBm
p_D	-25dBm

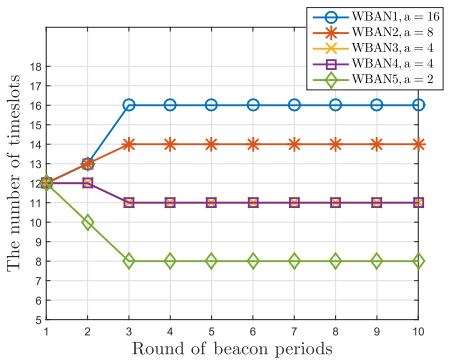

FIGURE 7. An example of timeslot allocation results.

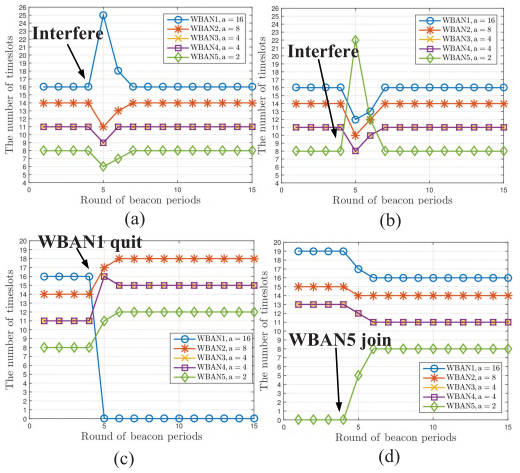

FIGURE 8. Convergency performance of the timeslot allocation game. (a)A WBAN with large value of *a* is required to demand the maximum number of timeslots in one beacon period. (b)A WBAN with small value of *a* is required to demand the maximum number of timeslots in one beacon period. (c)A WBAN quit the coexisting. (d)A WBAN join in the coexisting.

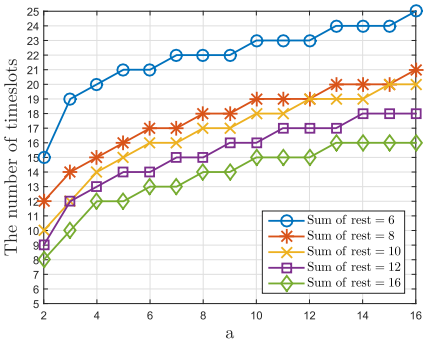

FIGURE 9. Variation trend of allocated timeslots under different values of *a*.

the coexisting scenario converge to the equilibrium state in 3 rounds of beacon periods from the initial state. Also, it can be observed that more timeslots are allocated to the WBANs with larger value of a which stands for more important individual or higher priority.

Fig. 8 illustrates the convergence performance of the proposed timeslot allocation game in different scenarios that possibly appear in reality. Fig. 8(a) and (b) present the condition when one coexisting WBAN needs a burst for more timeslots than its stable state. It can be seen from the figure that when the burst occurs, more timeslots are allocated to the corresponding WBAN in the following one beacon period while slots for other coexisting WBANs are cut. However, after the burst, coexisting WBANs converge back to the equilibrium state soon in 2 rounds of beacon periods. Fig. 8(c) and (d) demonstrate the conditions when one WBAN leaves and new WBAN joins. It can be indicated from the figure that equilibrium state are always converged to soon after the quitting and joining procedure. In summary, the timeslot allocation game is stable and can converge back to the equilibrium state fast when interferes happen among the coexisting WBANs.

In addition to this timeslot allocation game, the variation trend of allocated timeslots for a single WBAN under different values of a is investigated and the simulation results are shown in Fig. 9. Each curve in the figure is obtained in the coexisting scenario where, except for the investigated WBAN, the sum value of a in rest coexisting WBANs is designated. It can be seen from Fig. 9 that with the increasing value of a, the allocated timeslots for the investigated WBAN becomes larger and that the increasing trend slows down when the value of a is large. Also, the WBAN with same value of a get more timeslots in the environment where the sum of rest a is lower.

To conclude from the simulation results, the timeslot allocation game can provide differentiated timeslots for the coexisting WBANs according to the values of a that stands for priority and disease severity of an individual and the game can fast converge to a stable equilibrium state. Furthermore, the game also has the ability to recover back to the stable state

when suffering from the interferes like burst request, WBAN joining and WBAN quitting.

Next, we evaluate the performance of the proposed coexisting scheme in terms of transmission reliability, throughput, energy efficiency and transmission delay via the comparison with the original coexisting mechanism specified in IEEE 802.15.6. The reason why we choose the coexisting mechanism specified in IEEE 802.15.6 are listed as follows:

- Our proposed coexisting mechanism is an integrated scheme to address the coexisting problem in terms of channel access (multi-channel utilization), timeslot allocation, active period scheduling and transmission power control. While state-of-art schemes only concentrated on either multi-channel technology, timeslot allocation or power control. When implementing these schemes into the simulations, several aspects will be uncertain. For example, power control methods lacked timeslot allocation and scheduling, timeslot allocation methods were unable to decide transmission power and multi-channel methods only focused on multi-channel utilization to mitigate inter-BAN interference but did not coordinate the concurrent transmission in a single channel. As a result, we can not make up these lacking functions to these coexisting schemes and then make comparison with our proposal.
- Although literature [24] designed an integrated coexisting scheme for WBAN coexisting problem, the system model used in the literature was very different from the one used in this paper which is a more realistic system model than the model used in [24]. As a result, the integrated scheme in [24] can not work in our system model. Therefore, we are unable to use this scheme as a comparing scheme to evaluate our proposed mechanism.

For the reliability performance evaluation, we set the reuse factor $\theta = 2$ in the simulation and compare the outage probability under different SINR thresholds. The comparison results are drawn in Fig. 10. It can be indicated that with the increasing value of SINR threshold, the outage probability becomes obviously higher for all the curves. However, our proposed scheme performs better than the original coexisting scheme for the less outage probability. The advantage is more significant when the SINR threshold is higher. That is, when SINR threshold is -10dB, the advantage gap between our proposed scheme and the original mechanism is at least 0.6% while the gap enhances to 16% when the threshold rises to 25dB. In a word, coexisting WBANs with our proposed scheme transmit with higher reliability since less transmissions are failed to satisfy the reception requirements. Another interesting observation is that the impact of transmitting power on outage probability for the original mechanism is weak. The reason can be referred to Eq. (2) that increasing transmitting power for WBANs not only enlarges their own packets power but also raises the interference for other WBANs. The small differences between three curves without our scheme are caused by the packet RSSI value requirement. Larger transmitting power brings larger RSSI values which

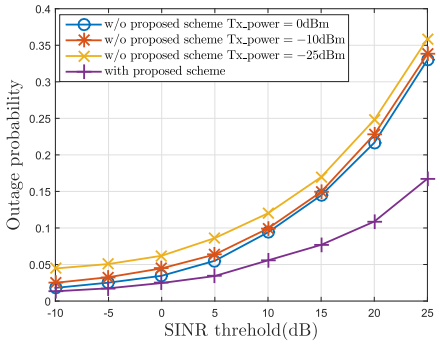

FIGURE 10. Reliability performance comparison.

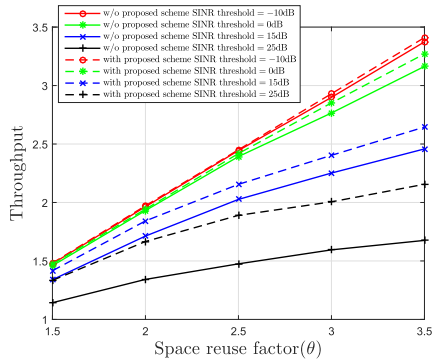

FIGURE 11. Throughput performance comparison.

are more possible to satisfy the RSSI threshold requirement in the packet reception.

The throughput comparison is illustrated in Fig. 11. The throughput we utilize in the figure is defined as the total number of successful transmitting packets of all coexisting WBANS per slot. The transmitting power of the original coexisting mechanism is set to maximum value (0dBm) which provides the best reliability for transmitting in the comparison. It can be seen from the figure that with the higher space reuse factor, the throughput increases since more packets can be sent concurrently in one time slot. Also, it can be known that no matter how SINR threshold varies, the proposed scheme is able to provide higher throughput than the original mechanism. It is because our proposed scheme provides higher reliability in the coexisting transmissions especially when the space reuse factor is high.

For clearer illustration, we draw the outage performance under different values of space reuse factor in Fig. 12. It can be seen from the figure that with the increasing value of reuse factor, the outage probability becomes higher, even more than 50% when $\theta = 3.5$ since more WBANs are transmitting at the same time. As a result, although higher space reuse factor brings about better throughput performance, it is unavailable in the coexisting scenario due to the extremely low reliability performance. However, our proposed scheme provides much better performance especially when the factor value is high. This advantage owes to the fact that our proposed scheme coordinates the active period of each coexisting WBAN and

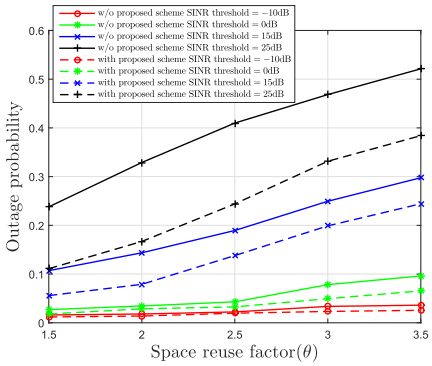

FIGURE 12. Outage performance under different space reuse factor.

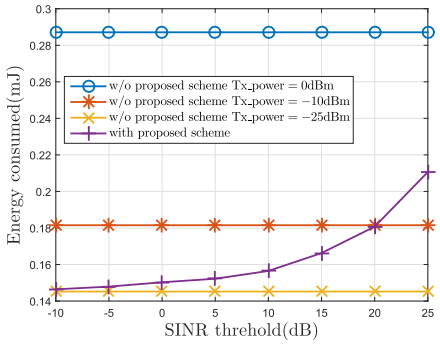

FIGURE 13. Energy consumed per transmission performance comparison.

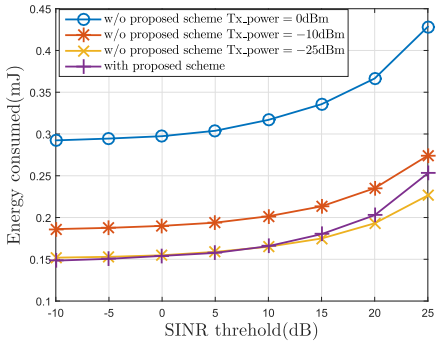

FIGURE 14. Energy consumed per successful transmission performance comparison.

selects an appropriate transmitting power to satisfy the reception requirement. On the other hand, the original one randomly selects the active period for each WBAN without the coordination which results in the possibly more concurrent transmissions causing large inter-BAN interference.

Inferred from Fig. 11 and 12, in our proposed coexisting mechanism, the value of θ can be adjusted according to the transmission requirements of the coexisting WBANs. For instance, θ can be set high if the transmissions of coexisting WBANs demand for high transmission rate but pay less attention on reliability, or it should be set a small value if the transmissions are error-sensitive with low transmission rate.

Finally, we evaluate the energy efficiency performance of the proposed scheme in terms of the energy consumed per transmission and the energy consumed per successful transmission. In the comparisons, we set θ to 2. Fig. 13 illustrates the comparison on energy consumed per transmission from the simulation. It can be indicated that with the increasing value of SINR threshold, the energy consumed per transmission of our proposed scheme becomes higher. It is because the transmission power of our scheme is decided based on the SINR threshold referring to Algorithm 3. It can also been seen that compared with the original mechanism with the maximum transmitting power, our proposed scheme realizes higher energy efficiency. It is because our proposed scheme utilizes power control to satisfy reception requirements with possible minimum power based on mobility prediction of coexisting WBANs and active scheduling results. Although the original mechanism with -10dBm and -25dBm transmitting power consume less energy when SINR threshold is relative high, they provide much lower reliability as shown in Fig. 10.

To evaluate the energy efficiency more reasonably, we portray the energy consumed per successful transmission performance in Fig. 14. It can be indicated from the figure that our proposed scheme has much better energy efficiency than the original mechanism with maximum power and also excels the one with -10dBm. When comparing with the original mechanism with the minimum power (-25dBm), the performance of our scheme is almost the same when SINR threshold is lower than 15dB and a little higher when SINR threshold is over 15dB. Specifically, the energy consumed per successful transmission of our scheme is higher than the original one with -25dBm power by 9.6% when SINR threshold is 25dB. However, the original one with minimum power provides 35% outage probability for the transmission which is much higher than our proposed scheme by 15.9%.

In addition to the performance evaluation of our proposed coexisting mechanism, we also design another simulation scenario based on the coexisting scenario described in Section III-A to observe the scalability and load sensitivity of our proposal. In this simulation scenario, the room size is still 6m$\times$6m while the total number of coexisting WBANs varies during the simulation. Each WBAN requires 8 transmission timeslots in one beacon period. The space reuse factor θ adjusts during the simulation according to the total required timeslots from all the coexisting WBANs. For example, when the number of coexisting WBANs is 5, the total required timeslots is $5 \times 8 = 40$. Then, θ is set to $40/30 = 4/3$. On the contrary, when the number of coexisting WBANs is less than 4, θ is set to 1 since the total number of required timeslots is less than 30 which is the total number of timeslots in one beacon period.

Fig. 15 illustrates the outage probability comparison under varying number of coexisting WBANs. The transmission power of the original mechanism is set to 0dBm as the same reason with Fig. 12. It can be seen from the figure

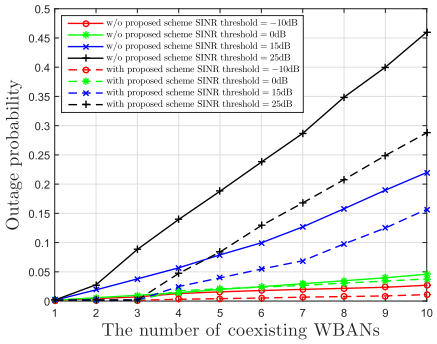

FIGURE 15. Outage probability performance comparison under varying number of WBANs.

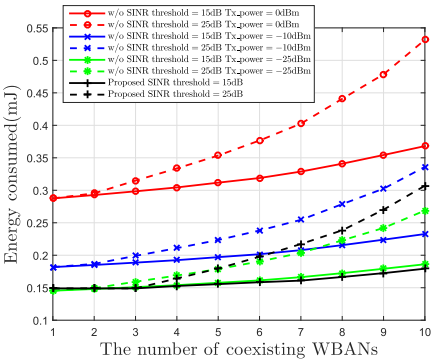

FIGURE 16. Energy consumed per successful transmission performance comparison under varying number of WBANs.

that with the increasing number of WBANs, the outage probability becomes higher for all the curves. It is because more coexisting WBANs bring larger inter-WBAN interference leading to more transmission failures. However, regardless of co-WBANs numbers and SINR threshold, our proposed mechanism always performs better than the original coexisting scheme for the less outage probability and the advantages becomes more significant when the number of coexisting WBANs increases. Also, as the same trend presented in Fig. 10, the performance gap between our proposal and the original coexisting mechanism becomes larger when the SINR threshold turns higher. Specifically, When the number of coexisting WBANs is 10 and the SINR threshold is set to 25dBm, the gap between our proposed coexisting mechanism and the original one can be as large as 18%. The reason for this advantage trend is that with the increasing number of WBANs, more transmission will be concurrently occurred and more inter-BAN interference is produced. In this case, active period coordination and the transmission power control becomes more important in concurrent transmission control and inter-BAN interference mitigation, which results in higher transmission reliability.

To analyze the energy efficiency of our proposed mechanism under varying number of coexisting WBANs, we draw the energy consumed per successful transmission performance in Fig. 16. It can be obviously seen from the figure that more energy will be cost for a successful transmission when the number of coexisting WBANs increases. It is because larger number of coexisting WBANs brings more inter-BAN interference and therefore incurs higher transmission outage probability. Also, when SINR threshold is set to 15dBm, our proposal has the lowest energy cost for a successful transmission even compared with the original mechanism with minimum power. The reason is that although the original mechanism with minimum power(-25dBm) uses less amount of energy for a transmission than our proposal, its transmission outage probability is much higher than our coexisting mechanism resulting in larger energy cost for a successful transmission. When SINR threshold comes to 25dBm, the energy cost per successful transmission of our proposed mechanism is lower than the original mechanism with 0dBm power and −10dBm power. Comparing with the one with −25dBm power, our proposed mechanism costs higher when the number of WBANs exceeds 5 and the largest gap is 12.1% when the number of co-WBANs is 10. However, in this case, the original one with minimum power provides 18% more transmission failures than our proposed mechanism.

In a word, when the total number of coexisting WBANs varies, our proposed mechanism can always provide higher transmission reliability when compared with the original coexisting mechanism specified in IEEE 802.15.6. The advantage becomes more significant when the number of co-WBANs increases. At the same time, our proposed mechanism maintains a high level energy efficiency under such conditions.

Besides, in order to fully illustrate our mobility prediction based power control method in our proposed coexisting scheme, we compare the deviation relationship between the distance of one pair of coexisting WBANs and the transmitting power calculated in Algorithm 3 as shown in Fig. 17. The simulation settings for this illustration are the same with Fig.7-9. In the figure, the distance axis represents the distance between WBAN 1 and WBAN 3, while the transmission power index axis indicates the power level of WBAN 1 in the slots that WBAN 1 and WBAN 3 are concurrently transmitting. It can be seen from the figure that the transmission power level varies inversely with the distance. When the distance becomes large between the 5th to 10th beacon periods, WBAN 1 decreases its transmitting power. On the other hand, as the distance turns to be small between 15th to 30th beacon periods, WBAN 1 increases its power to guarantee the SINR requirement. The unusual mutation of the transmission power in 24th period in the figure is caused by the shadowing effect that the path loss between WBAN 1 and WBAN 3 is blocked by their own bodies or other coexisting WBANs. In a word, our mobility prediction based power control method is able to adjust the transmitting power according to the mobility conditions of coexisting WBANs.

At the end of the evaluation, delay performance of our proposed coexisting mechanism is also discussed. The Frame Generation Interval(FGI) of each coexisting WBAN and its

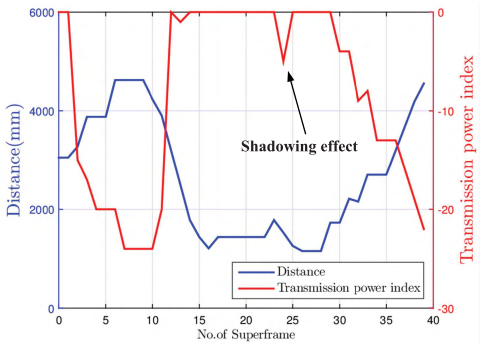

FIGURE 17. Deviation relationship between distance and transmission power.

TABLE 5. Frame generation interval of each coexisting WBAN and its corresponding parameter *a*.

	WBAN1	WBAN2	WBAN3	WBAN4	WBAN5
FGI(ms)	25	30	40	40	60
a	16	8	4	4	2

corresponding parameter a are listed in Table 5. Short FGI of a WBAN means large traffic flow rate in this WBAN and therefore, its parameter a has a large value. To obtain delay performance, the SINR threshold in the simulations is set to $5dB$ and the space reuse factor is set to 2. Any frames which have been waiting over 500ms in the transmitting queue will be abandoned since outdated information is useless in medical applications. When a frame suffers from transmission failure, it can be retransmitted in the next beacon period. In order to present the advantage of individual differentiation of our proposed coexisting mechanism, average timeslot allocation method is also involved in the simulation as a comparing method.

The delay performance comparison is illustrated in Fig. 18. It can be seen from the figure that all of the coexisting WBANs under our proposed mechanism have the lowest delay comparing with other two methods. The delay of the original coexisting mechanism is a little bit higher than our proposal owing to the fact that the original one has lower transmission reliability resulting in more frame retransmission which will incur more delay. When comparing with average timeslot allocation method, it can be obviously observed that WBAN1 under average method has an excessive larger delay than other coexisting WBANs while the delay of WBAN1 under our proposal is in the same range with other WBANs. It is because average method allocate timeslots to each coexisting WBAN equally regardless of priorities and actual requirements of these WBANs. In this condition, WBANs with small requirements can't fully use these allocated slots while WBAN1 doesn't obtain enough timeslots for its frame transmission. As a result, WBAN1 acquires a very high delay while other coexisting WBANs obtain very low delay. Furthermore, many frames in WBAN1 are dropped as these frames have waited in the transmission queue over

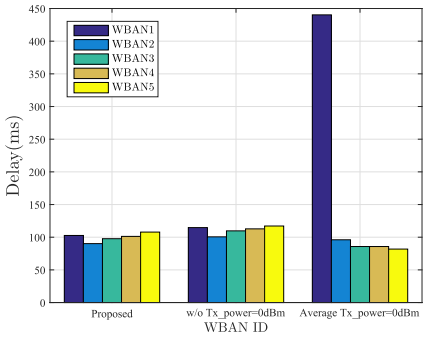

FIGURE 18. Delay performance comparison.

TABLE 6. Frame drop ratio performance comparison.

FDR(%)	WBAN1	WBAN2	WBAN3	WBAN4	WBAN5
Proposal	0.0013	0.0016	0.0015	0.0015	0.0018
Original	0.0159	0.0175	0.0187	0.0187	0.0138
Average	10.6600	0.0016	0.0015	0.0015	0.0005

500ms. The Frame Drop Ratio(FDR) obtained from the simulations in Table 6 can present this phenomenon. On the contrary, in our proposal, each coexisting WBAN is allocated according to its priority and requirement related parameter a, which is more rational and consequently results in satisfying delay performance.

To conclude the performance evaluation, our proposed coexisting mechanism can make differentiated timeslot allocation for each coexisting WBAN according to their requirements or priority in a distributed way and it is stable and convergent in abnormal situations. Compared with the original coexisting mechanism specified in IEEE 802.15.6, our proposed scheme can effectively improve the transmission reliability, network throughput, transmission delay and at the same time guarantee a high level energy efficiency.

VII. CONCLUSION

In this paper, an individual differentiated coexisting mechanism has been proposed for multiple-WBANs coexisting. The proposed mechanism consists of four parts, which are Timeslot allocation, Access control, Active period scheduling and Power control. Specifically, the timeslot allocation is designed based on game theory. We have proved the existence and uniqueness of Nash equilibrium for this game and derive a rapid distributed algorithm to find the equilibrium point. The simulation results demonstrate that our proposed mechanism has the ability to allocate different number of timeslots to each WBAN in a distributed and convergent way depending on their priorities and requirements. Furthermore, compared to the original coexisting methods in IEEE 802.15.6, our proposed mechanism can effectively improve the transmission reliability, network throughput, energy efficiency and transmission delay as well.

Our future work is to conduct experiments to test the validity and performance of our proposal on real WBAN platform. Furthermore, as there are still potentials in each part of our coexisting mechanism, we will attempt to revise and improve each of these parts in the future.

REFERENCES

[1] R. Cavallari, F. Martelli, R. Rosini, C. Buratti, and R. Verdone, "A survey on wireless body area networks: Technologies and design challenges," *IEEE Commun. Surveys Tuts.*, vol. 16, no. 3, pp. 1635–1657, 3rd Quart., 2014.

[2] D. Jiang, W. Li, and H. Lv, "An energy-efficient cooperative multicast routing in multi-hop wireless networks for smart medical applications," *Neurocomputing*, vol. 220, pp. 160–169, Jan. 2017.

[3] D. Jiang, Y. Wang, Y. Han, and H. Lv, "Maximum connectivity-based channel allocation algorithm in cognitive wireless networks for medical applications," *Neurocomputing*, vol. 220, no. 12, pp. 41–51, 2017.

[4] M. Ali, H. Moungla, M. Younis, and A. Mehaoua, "Distributed scheme for interference mitigation of WBANs using predictable channel hopping," in *Proc. IEEE Healthcom*, Sep. 2016, pp. 1–6.

[5] S. Kim, S. Kim, J.-W. Kim, and D.-S. Eom, "A beacon interval shifting scheme for interference mitigation in body area networks," *Sensors*, vol. 12, no. 8, pp. 10930–10946, 2012.

[6] J. Dong and D. Smith, "Cooperative body-area-communications: Enhancing coexistence without coordination between networks," in *Proc. IEEE PIMRC*, Sep. 2012, pp. 2269–2274.

[7] W. Huang and T. Q. S. Quek, "Adaptive CSMA/CA MAC protocol to reduce inter-WBAN interference for wireless body area networks," in *Proc. IEEE BSN*, Jun. 2015, pp. 1–6.

[8] Y. Xiao, X. Shan, and Y. Ren, "Game theory models for IEEE 802.11 DCF in wireless ad hoc networks," *IEEE Commun. Mag.*, vol. 43, no. 3, pp. S22–S26, Mar. 2005.

[9] A. Babaei and B. Jabbari, "Transmission probability control game for coexisting random ALOHA wireless networks in unlicensed bands," in *Proc. IEEE VTC*, May 2010, pp. 1–5.

[10] Y. Hou, M. Li, and D. Yang, "A game theoretical approach to coexistence of heterogeneous MIMO wireless networks with interference cancellation," in *Proc. IEEE ICNC*, Feb. 2016, pp. 1–5.

[11] Y. Hou, M. Li, X. Yuan, Y. T. Hou, and W. Lou, "Cooperative interference mitigation for heterogeneous multi-hop wireless networks coexistence," *IEEE Trans. Wireless Commun.*, vol. 15, no. 8, pp. 5328–5340, Aug. 2016.

[12] B. Guler and A. Yener, "Uplink interference management for coexisting MIMO femtocell and macrocell networks: An interference alignment approach," *IEEE Trans. Wireless Commun.*, vol. 13, no. 4, pp. 2246–2257, Apr. 2014.

[13] M. F. Yaqub, A. Haider, I. Gondal, and J. Kamruzzaman, "Self and static interference mitigation scheme for coexisting wireless networks," *Comput. Elect. Eng.*, vol. 40, no. 2, pp. 307–318, 2014.

[14] H. Lee, H. Kwon, A. Motskin, and L. Guibas, "Interference-aware MAC protocol for wireless networks by a game-theoretic approach," in *Proc. IEEE INFOCOM*, Apr. 2009, pp. 1854–1862.

[15] *IEEE Standard for Local and Metropolitan Area Networks—Part 15.6: Wireless Body Area Networks*, IEEE Standard 802.15.6-2012, Feb. 2012, pp. 1–271.

[16] S. Cheng, C. Huang, and C. C. Tu, "RACOON: A multiuser QoS design for mobile wireless body area networks," *J. Med. Syst.*, vol. 35, no. 5, pp. 1277–1287, 2011.

[17] A. Natarajan, M. Motani, B. de Silva, K.-K. Yap, and K.-C. Chua, "Investigating network architectures for body sensor networks," in *Proc. HealthNet*, 2007, pp. 19–24.

[18] B. de Silva, A. Natarajan, and M. Motani, "Inter-user interference in body sensor networks: Preliminary investigation and an infrastructure-based solution," in *Proc. BSN Workshop*, 2009, pp. 35–40.

[19] S. L. Cotton, W. G. Scanlon, and P. S. Hall, "A simulated study of co-channel inter-BAN interference at 2.45 GHz and 60 GHz," in *Proc. Eur. WTC*, 2010, pp. 61–64.

[20] B. Kim, J. Cho, D.-Y. Kim, and B. Lee, "ACESS: Adaptive channel estimation and selection scheme for coexistence mitigation in WBANs," in *Proc. IMCOM*, 2016, Art. no. 96.

[21] H. Moungla, K. Haddadi, and S. Boudjit, "Distributed interference management in medical wireless sensor networks," in *Proc. IEEE CCNC*, Jan. 2016, pp. 1–5.

[22] B. Kim, J.-H. Choi, and J. Cho, "A hybrid channel access scheme for coexistence mitigation in IEEE 802.15.4-Based WBAN," *IEEE Sensors J.*, vol. 17, no. 21, pp. 7189–7195, Nov. 2017.

[23] M. Ali, H. Moungla, M. Younis, and A. Mehaoua, "Inter-WBANs interference mitigation using orthogonal Walsh Hadamard codes," in *Proc. IEEE PIMRC*, Sep. 2016, pp. 1–7.

[24] S. Movassaghi, A. Majidi, A. Jamalipour, D. Smith, and M. Abolhasan, "Enabling interference-aware and energy-efficient coexistence of multiple wireless body area networks with unknown dynamics," *IEEE Access*, vol. 4, pp. 2935–2951, Jun. 2016.

[25] C.-J. Lee and J.-R. Lee, "QoS-based interference mitigation scheme in wireless body area networks," in *Proc. IEEE ICTC*, Oct. 2017, pp. 610–615.

[26] L. Zou, B. Liu, C. Chen, and C. W. Chen, "Bayesian game based power control scheme for inter-WBAN interference mitigation," in *Proc. IEEE Globecom*, Dec. 2014, pp. 240–245.

[27] D. Du, F. Hu, F. Wang, Z. Wang, Y. Du, and L. Wang, "A game theoretic approach for inter-network interference mitigation in wireless body area networks," *China Commun.*, vol. 12, no. 9, pp. 150–161, Sep. 2015.

[28] E. Forrister, G. Lee, D. Xue, B. Garner, and Y. Li, "Characterization of narrowband on-body wireless channels using motion capture experimentation," in *Proc. IEEE WMCS*, Mar./Apr. 2016, pp. 1–4.

[29] A. Ruaro, J. Thaysen, and K. B. Jakobsen, "Head-centric body-channel propagation paths characterization," in *Proc. IEEE EuCAP*, Apr. 2015, pp. 1–4.

[30] M. Ghandi, E. Tanghe, W. Joseph, M. Benjillali, and Z. Guennoun, "Path loss characterization of horn-to-horn and textile-to-textile on-body mmWave channels at 60 GHz," in *Proc. IEEE WINCOM*, Oct. 2016, pp. 235–239.

[31] D. Goswami, K. C. Sarma, and A. Mahanta, "Path loss variation of on-body UWB channel in the frequency bands of IEEE 802.15.6 standard," *Healthcare Technol. Lett.*, vol. 3, no. 2, pp. 129–135, Jun. 2016.

[32] N. Bhargav, S. L. Cotton, G. A. Conway, A. McKernan, and W. G. Scanlon, "Simultaneous channel measurements of the on-body and body-to-body channels," in *Proc. IEEE PIMRC*, Sep. 2016, pp. 1–6.

[33] F. Mani and R. D'Errico, "A spatially aware channel model for body-to-body communications," *IEEE Trans. Antennas Propag.*, vol. 64, no. 8, pp. 3611–3618, Aug. 2016.

[34] S. J. Ambroziak, L. M. Correia, and K. Turbic, "Radio channel measurements in body-to-body communications in different scenarios," in *Proc. IEEE URSI AP-RASC*, Aug. 2016, pp. 1376–1379.

[35] M. Cheffena and M. Mohamed, "The application of lognormal mixture shadowing model for B2B channels," *IEEE Sensors Lett.*, vol. 2, no. 3, Sep. 2018, Art. no. 7500704.

[36] M. D. Pereira, G. A. Alvarez-Botero, and F. R. de Sousa, "Characterization and modeling of the capacitive HBC channel," *IEEE Trans. Instrum. Meas.*, vol. 64, no. 10, pp. 2626–2635, Oct. 2015.

[37] Y. Zhang, Z. He, Y. Liu, L. A. L. Enamorado, and X. Chen, "Measurement and characterization on a human body communication channel," in *Proc. IEEE PIMRC*, Sep. 2016, pp. 1–6.

[38] Z. Cai, M. Seyedi, G. Z. Zhang, R. Li, D. T. H. Lai, and Q. Ye, "Preliminary characterization of impulse radio intrabody communication," in *Proc. IEEE TENCON*, Nov. 2015, pp. 1–6.

[39] D. Jiang, Z. Xu, W. Li, C. Yao, Z. Lv, and T. Li, "An energy-efficient multicast algorithm with maximum network throughput in multi-hop wireless networks," *J. Commun. Netw.*, vol. 18, no. 5, pp. 713–724, 2016.

[40] *Castalia: A Simulator for Wireless Sensor Networks and Body Area Networks. User's Manual*. Australia's Information and Communications Technology Research Center (NICTA), Sydney, NSW, Australia, 2011.

[41] D. Smith, L. Hanlen, J. Zhang, D. Miniutti, D. Rodda, and B. Gilbert, "First- and second-order statistical characterizations of the dynamic body area propagation channel of various bandwidths," *Ann. Telecommun.*, vol. 66, no. 3, pp. 187–203, 2011.

[42] D. Fugenberg and J. Tirole, *Game Theory*. Cambridge, MA, USA: MIT Press, 1991.

[43] V. Berinde, *Iterative Approximation of Fixed Points*. Berlin, Germany: Springer, 2007.

[44] Chipcon. *CC2420: 2.4 GHz IEEE 802.15.4/ZigBee-Ready RF Transceiver*. Accessed: 2015. [Online]. Available: http://www.chipcon.com

BING ZHANG was born in 1970. He received the B.S., M.S., and Ph.D. degrees from Xidian University, Xi'an, China, in 1992, 1995, and 2008, respectively. He is currently a Professor with the State Key Laboratory of Integrated Services Networks, Xidian University. His research interests are in the areas of broadband networks and switching, broadband access networks, and home networking, communication network protocol design, and Internet Quality of Services.

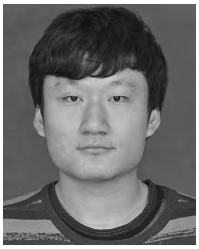

YU ZHANG was born in 1990. He received the B.S. degree in telecommunication engineering from Xidian University, China, in 2012. He is currently pursuing the Ph.D. degree with the School of Telecommunications Engineering, Xidian University, Xi'an, China. His research interests are in the areas of wireless body area networks.